nature medicine

Glutaminyl cyclase inhibition attenuates pyroglutamate Aβ and Alzheimer's disease–like pathology

Stephan Schilling[1], Ulrike Zeitschel[2], Torsten Hoffmann[1], Ulrich Heiser[1], Mike Francke[2], Astrid Kehlen[1], Max Holzer[2], Birgit Hutter-Paier[3], Manuela Prokesch[3], Manfred Windisch[3], Wolfgang Jagla[4], Dagmar Schlenzig[1], Christiane Lindner[5], Thomas Rudolph[5], Gunter Reuter[5], Holger Cynis[1], Dirk Montag[6], Hans-Ulrich Demuth[1,4] & Steffen Rossner[2]

Because of their abundance, resistance to proteolysis, rapid aggregation and neurotoxicity, N-terminally truncated and, in particular, pyroglutamate (pE)-modified Aβ peptides have been suggested as being important in the initiation of pathological cascades resulting in the development of Alzheimer's disease[1–6]. We found that the N-terminal pE-formation is catalyzed by glutaminyl cyclase *in vivo*. Glutaminyl cyclase expression was upregulated in the cortices of individuals with Alzheimer's disease and correlated with the appearance of pE-modified Aβ. Oral application of a glutaminyl cyclase inhibitor resulted in reduced $Aβ_{3(pE)–42}$ burden in two different transgenic mouse models of Alzheimer's disease and in a new *Drosophila* model. Treatment of mice was accompanied by reductions in $Aβ_{x–40/42}$, diminished plaque formation and gliosis and improved performance in context memory and spatial learning tests. These observations are consistent with the hypothesis that $Aβ_{3(pE)–42}$ acts as a seed for Aβ aggregation by self-aggregation and co-aggregation with $Aβ_{1–40/42}$. Therefore, $Aβ_{3(pE)–40/42}$ peptides seem to represent Aβ forms with exceptional potency for disturbing neuronal function. The reduction of brain pE-Aβ by inhibition of glutaminyl cyclase offers a new therapeutic option for the treatment of Alzheimer's disease and provides implications for other amyloidoses, such as familial Danish dementia.

The brains of individuals with Alzheimer's disease are characterized by the presence of neurofibrillary tangles and by deposits of Aβ in neocortical brain structures[1]. Sequential β- and γ-secretase cleavage of the amyloid precursor protein (APP) liberates Aβ peptides, which have different amyloidogeneity and neurotoxicity[1–3]. Glutamate at the N-terminus of truncated Aβ can be subsequently cyclized into pE, resulting in $Aβ_{3(pE)–40/42}$ (refs. 4–6) and $Aβ_{11(pE)–40/42}$ (refs. 7,8). This pE-modification of Aβ confers proteolytic resistance[9,10] and loss of N-terminal charge, resulting in accelerated aggregation of $Aβ_{3(pE)}$ compared with unmodified Aβ[11]. In particular, $Aβ_{3(pE)–42}$, a major constituent of Aβ deposits in sporadic and familial Alzheimer's disease[4,12], is neurotoxic[9]. Thus, reduction of $Aβ_{3(pE)–42}$ should promote Aβ proteolysis and could, in turn, prevent Aβ aggregation by clearance of a major nucleation factor and thereby enhance neuronal survival. Recently, we discovered that glutaminyl cyclase is capable of catalyzing $Aβ_{3(pE)–42}$ formation and that glutaminyl cyclase inhibitors prevent $Aβ_{3(pE)–42}$ generation *in vitro*[13,14]. Here, we asked whether glutaminyl cyclase expression is altered in the Alzheimer's disease brain and might therefore be involved in the generation of $Aβ_{3(pE)}$ *in vivo* and whether chronic glutaminyl cyclase inhibition affects Aβ deposition, gliosis and memory deficits in animal models of Alzheimer's disease.

Glutaminyl cyclase is widely distributed in mammalian brain with considerable expression in the hippocampus and cortex[15,16]. To assess whether glutaminyl cyclase expression can be correlated with the generation of $Aβ_{3(pE)–42}$ in Alzheimer's disease, we analyzed glutaminyl cyclase mRNA and protein concentrations in human neocortical brain samples post mortem (**Fig. 1a**,**b**). Glutaminyl cyclase mRNA and protein were upregulated in samples from individuals with Alzheimer's disease compared with samples from normal aging individuals. Moreover, significantly larger concentrations of $Aβ_{3(pE)–42}$ were detected in samples from individuals with Alzheimer's disease compared with nondemented individuals, supporting a role for glutaminyl cyclase in the generation of $Aβ_{3(pE)–42}$ ($P < 0.05$; **Fig. 1c**). In contrast, ELISA analysis also revealed high total $Aβ_{x–42}$ concentrations in aged controls (**Fig. 1c**). This observation was corroborated by immunohistochemistry (**Fig. 1d**). Aβ immunoreactivity was detected in the brain sections of all groups. In contrast, $Aβ_{3(pE)–42}$ staining was absent in normal aging but was specific for Alzheimer's disease brain, where $Aβ_{3(pE)–42}$ immunoreactivity was almost as high as total Aβ.

To substantiate the correlation of glutaminyl cyclase expression and $Aβ_{3(pE)–42}$ generation, we co-expressed APP and glutaminyl cyclase in HEK293 cells. Glutaminyl cyclase strongly accelerated the generation of $Aβ_{3(pE)–42}$. The $Aβ_{3(pE)–42}$ formation is suppressed in a

[1]Probiodrug AG, Weinbergweg 22, 06120 Halle/S., Germany. [2]Paul Flechsig Institute for Brain Research, University of Leipzig, Jahnallee 59, 04109 Leipzig, Germany. [3]JSW-CNS Research GmbH, Parkring 12, 8074 Grambach/Graz, Austria. [4]Ingenium Pharmaceuticals GmbH, Fraunhoferstrasse 13, 82152 Munich-Martinsried, Germany. [5]Institute of Biology, Department of Genetics, University of Halle-Wittenberg, Weinbergweg 10, 06120 Halle/S., Germany. [6]Research Group Neurogenetics, Leibniz Institute for Neurobiology, Brenneckestrasse 6, 39118 Magdeburg, Germany. Correspondence should be addressed to H.-U.D. (hans-ulrich.demuth@probiodrug.de).

Received 12 March; accepted 3 September; published online 28 September 2008; doi:10.1038/nm.1872

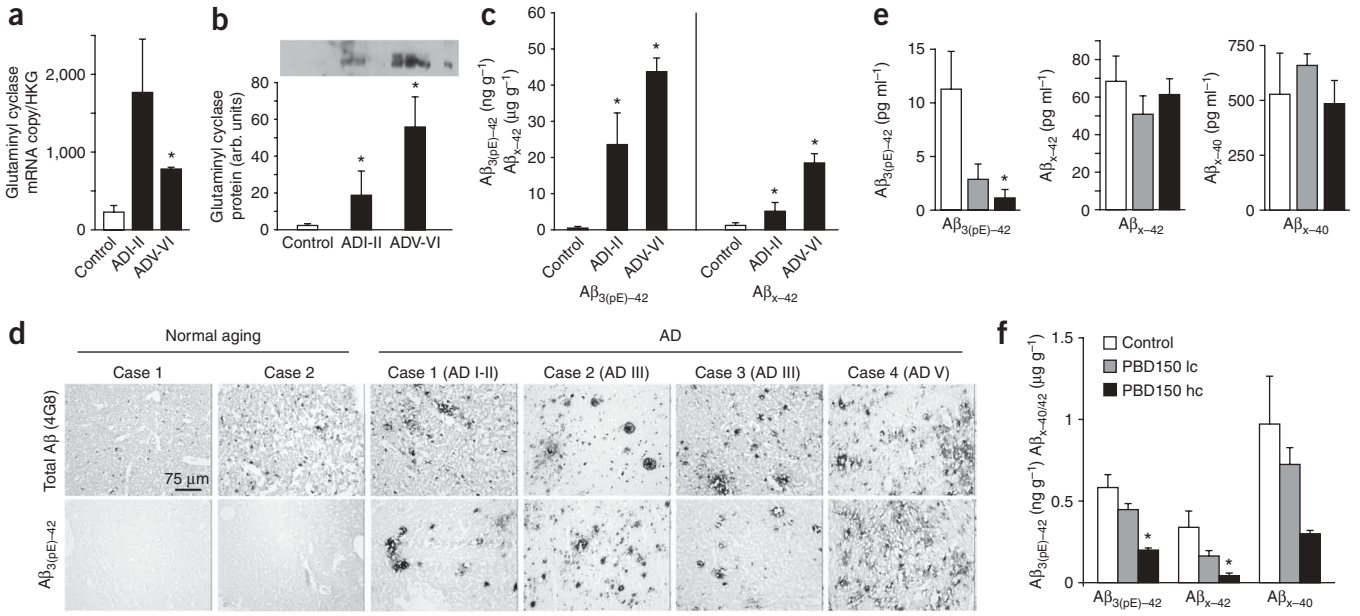

Figure 1 Glutaminyl cyclase expression and pE-Aβ in Alzheimer's disease: prevention of pE-Aβ formation by glutaminyl cyclase inhibition *in vitro* and *in vivo*. (**a**) Quantitative analysis of glutaminyl cyclase transcript levels. Total RNA from human neocortical brain samples (Brodmann area 22) was isolated from aged controls and individuals with Alzheimer's disease (Braak stages are indicated with Roman numerals). (**b**) Western blot analysis of the same cases and brain region as used for glutaminyl cyclase mRNA analysis. (**c**) Quantification of $A\beta_{3(pE)–42}$ and of $A\beta_{1–42}$ concentrations from the samples in **a** and **b**, using ELISA analysis. (**d**) Immunohistochemical detection of total Aβ peptides with 4G8 and of $A\beta_{3(pE)–42}$ peptides in Brodmann area 22 from aged controls and individuals with Alzheimer's disease. Sparse Aβ plaques were detected in normal aging, but these deposits lacked $A\beta_{3(pE)–42}$ immunoreactivity. (**e**) Quantification of Aβ concentrations in conditioned media of HEK293 cells, which were transiently transfected with an APPsw/l variant[29] and human glutaminyl cyclase. PBD150 was applied at 0.1 μM (low concentration, PBD150 lc) and 1 μM (high concentration, PBD150 hc) concentrations. The formation of $A\beta_{3(pE)–42}$, but not of $A\beta_{x–42}$ and $A\beta_{x–40}$, was significantly reduced, substantiating the specificity of PBD150. (**f**) Quantification of Aβ concentrations in the brains of 10-month-old Tg2576 control mice and of age-matched littermates treated for 6 months with PBD150 at a concentration of 2.4 mg (PBD150 lc) or 7.2 mg (PBD150 hc) per g of food pellets. Only female mice were enrolled in the study ($n = 4$ per group). Data are expressed as mean ± s.e.m. (* $P < 0.05$ versus control, one-way ANOVA followed by Tukey HSD).

dose-dependent manner by the glutaminyl cyclase inhibitor PBD150 (ref. 17). Notably, amyloidogenic processing was not influenced *per se*, as indicated by unchanged concentrations of $A\beta_{x–42}$ and $A\beta_{x–40}$, demonstrating the specific effect of the compound on glutaminyl cyclase catalysis (**Fig. 1e**).

PBD150 did not affect the activities of proteases involved in Aβ degradation (such as insulin-degrading enzyme, neutral endopeptidase or aminopeptidase N) and in Aβ generation (beta-site APP cleaving enzyme1) (**Supplementary Fig. 1** online).

Subsequently, we applied PBD150 orally to 4-month-old female Tg2576 mice for 6 months to study effects of glutaminyl cyclase inhibition on the concentrations of $A\beta_{3(pE)–42}$, $A\beta_{x–42}$ and $A\beta_{x–40}$ in the insoluble Aβ pool (**Supplementary Fig. 1**). The compound was administered via implementation into food pellets and reached brain concentrations of at least 0.02 μg per g of body weight, which corresponds to approximately half-maximal inhibition of glutaminyl cyclase. Pharmacokinetic evaluations gave no evidence for an accumulation of the compound in brain or other organs. Similar weight gain and mortality in treated and control groups indicated that PBD150 was well tolerated (data not shown).

We found a dose-dependent decrease of $A\beta_{3(pE)–42}$ by 23% for a low dose of PBD150 and by 65% for a high dose of PBD150 (**Fig. 1f**). $A\beta_{3(pE)–42}$ reduction alleviated $A\beta_{x–42}$ and $A\beta_{x–40}$ concentrations in a dose-dependent manner (**Fig. 1f**). These initial findings suggest that $A\beta_{3(pE)–42}$ generation is mediated by glutaminyl cyclase *in vivo* and that there is a relationship between $A\beta_{3(pE)–42}$ and the aggregation of total Aβ.

To assess whether glutaminyl cyclase inhibition could abrogate the accumulation of $A\beta_{3(pE)–42}$, $A\beta_{x–42}$ and $A\beta_{x–40}$, we initiated long-term treatment of Tg2576 mice at 6 months of age and continued it for 10 months. Tg2576 mice start to develop plaques by the age of 10–12 months. At the end of the study, untreated mice were expected to show profound plaque burden and behavioral impairment. The effects of PBD150 on total Aβ and $A\beta_{3(pE)–42}$ essentially resembled those seen in the younger mice treated from months 4 to 10. The reduction of $A\beta_{3(pE)–42}$ by 26% and 52% after application of PBD150 at a low and high dose, respectively, was accompanied by a significant and dose-dependent lowering of $A\beta_{x–42}$ (by 45% and by 75%) and $A\beta_{x–40}$ (by 31% and by 66%) ($P < 0.05$; **Fig. 2a**).

Immunohistochemistry revealed diminished cortical plaque formation after PBD150 treatment (**Fig. 2b,c**). Moreover, the load of cored plaques detected by thioflavin-S staining was reduced by PBD150 treatment (**Fig. 2b**), again supporting a modulating role for $A\beta_{3(pE)–42}$ in Aβ aggregation. The decrease in plaque load was accompanied by alleviated plaque-associated inflammation, involving both glial fibrillary acidic protein (GFAP)-immunoreactive astrocytes and biotin-GSA–labeled microglial cells (**Fig. 2b**).

Notably, no significant differences in concentrations of soluble $A\beta_{x–40}$ or $A\beta_{x–42}$ were observed in any of the treatment procedures (analysis of variance (ANOVA), $F_{2,27} = 0.890$, $P = 0.423$, data not shown), effectively ruling out a direct effect of PBD150 on Aβ production. Similarly, the expression of APP and its secretory processing were not affected by glutaminyl cyclase inhibition in Tg2576 organotypic brain slice cultures (**Supplementary Fig. 2** online).

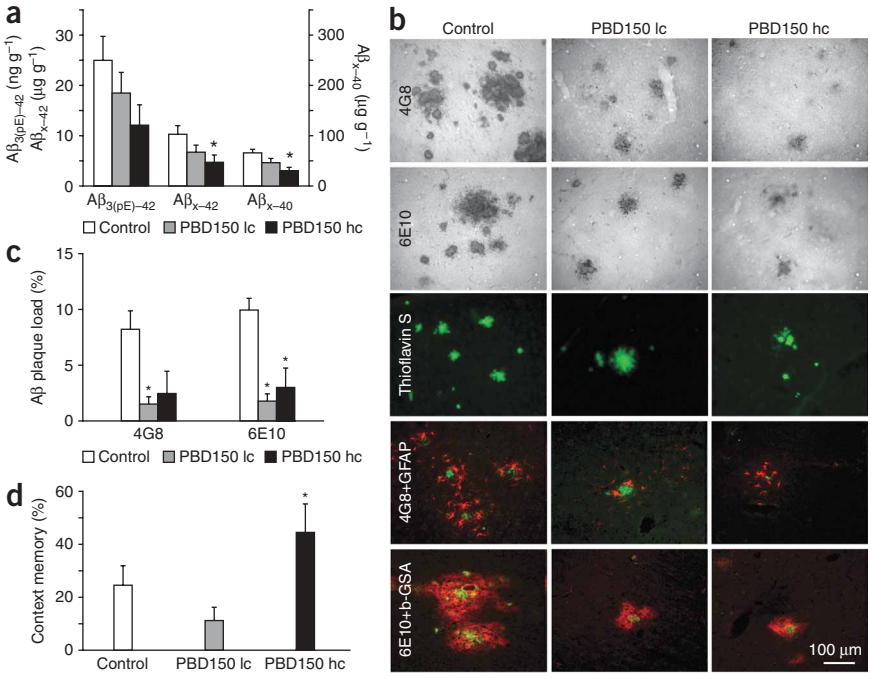

Figure 2 Effects of glutaminyl cyclase inhibition on Tg2576 mice. (**a**) Quantification of Aβ concentrations in the brains of 16-month-old Tg2576 control mice and of age-matched littermates treated for 10 months (prophylactic treatment) with PBD150 at a concentration of 2.4 mg (PBD150 lc) or 7.2 mg (PBD150 hc) per g of food pellets. Groups consisted of male and female mice ($n = 8$–12; control consisted of 5 females and 4 males, PBD150 hc consisted of 4 males and 4 females, PBD150 lc consisted of 6 males and 6 females). Data are expressed as mean ± s.e.m. (* $P < 0.05$ versus control, one-way ANOVA followed by Tukey HSD). (**b**) Immunohistochemical detection of Aβ plaques in 16-month-old control mice and of age-matched littermates treated for 10 months with PBD150, as described in **a**. Top, 3,3'-diaminobenzidine (DAB) staining of Aβ plaques with 4G8 and 6E10 antibodies. The reduced Aβ plaque burden was accompanied by diminished gliosis, as shown for the astrocytic (GFAP, red fluorescence) and microglial (bio-GSA, red fluorescence) labeling. The scale bar applies to all images. (**c**) The plaque load was significantly reduced, as shown by quantification of histochemical stainings. (**d**) Conditioned fear test performed at the end of the treatment period. When only female mice were analyzed, there was significantly improved context fear memory (% immobile in context – novel) in mice treated with the high dose of PBD150 (44.2%) as compared with the control group (24.4%) and with the low dose PBD150 group (11.2%, $P = 0.0158$; ANOVA, $F_{2,13} = 3.901$, $P = 0.0471$, $n = 5$–8). Data are expressed as mean ± s.e.m. (* $P < 0.05$ versus control, Fisher least-significant difference).

To evaluate the potential effect of glutaminyl cyclase inhibition on animal behavior, we applied a conditioned fear procedure as employed recently to monitor age-dependent changes of context memory in Tg2576 mice[18]. In female mice, improvement of context memory was observed in the high-dose PBD150 group (44.2%), as compared with the control group (24.4%) and with the low-dose PBD150 group (11.2%, $P = 0.0158$) (ANOVA, $F_{2,13} = 3.901$, $P = 0.0471$; **Fig. 2d**). Only female mice were analyzed, because the constitution of the groups for behavioral analysis was inconsistent with respect to gender. Freezing behavior before conditioning or in a novel environment with or without a cued tone was not different between treated and untreated mice (with tone: untreated, 67.6%; low dose, 61.3%; high dose, 90.6%; $F_{2,13} = 2.488$, $P = 0.1217$; without tone: untreated, 47.5%; low dose, 56.6%; high dose, 34.3%; $F_{2,13} = 0.753$, $P = 0.4904$), indicating an effect of PBD150 specifically on context memory.

To determine the efficacy of PBD150 in mice with distinct plaque pathology, we orally treated 10-month-old female Tg2576 mice with PBD150 for 6 months in a third trial. A moderate reduction of cortical $A\beta_{3(pE)–42}$ (by 26% and 43% compared to 100% of the control group) was observed on treatment without effect on $A\beta_{x–42}$ and $A\beta_{x–40}$ peptides and on the total plaque load (**Supplementary Fig. 3** online). The microglial activation around plaques was reduced, as observed in the prophylactic treatment study (see **Fig. 2b**). Contextual fear conditioning showed a tendency toward dose-dependent improvement of cognition in the treated animals (**Supplementary Fig. 3**), although this improvement was not statistically significant. Freezing behavior before conditioning or in a novel environment with or without a cued tone was not different between treated and untreated mice (with tone: untreated, 71.5%; low dose, 61.0%; high dose, 60.2%; $F_{2,19} = 0.415$, $P = 0.6663$; without tone: untreated, 41.4%; low dose, 38.5%; high dose, 38.0%; $F_{2,19} = 0.038$, $P = 0.9628$).

Taken together, the data of the three different studies in Tg2576 mice suggest that the *de novo* formation of $A\beta_{3(pE)–42}$ can be influenced by glutaminyl cyclase inhibition at any stage of the aggregation process, without substantial effect on previously formed deposits. This provides strong evidence for the concept of $A\beta_{3(pE)–42}$ acting as a seeding peptide species[11].

This conclusion was substantiated by PBD150 treatment of another transgenic mouse line, TASD-41, which is characterized by the neuron-specific overexpression of human APP751 with two familial Alzheimer's disease mutations (APP Swedish and APP London, APPsw/l mice). Because these mice develop Aβ plaques at 5 to 6 months of age, we treated them from months 4 to 7 with the high dose of PBD150 (7.2 mg per g food pellet), which was found to be efficient in Tg2576 mice. Similarly, PBD150 reduced the concentration of $A\beta_{3(pE)–42}$ by 58% and that of $A\beta_{x–42}$ and $A\beta_{x–40}$ by 61% and 54%, respectively (**Fig. 3a**). The plaque density in brains of TASD-41 mice was significantly diminished by 80% and accompanied by alleviated gliosis ($P < 0.05$; **Fig. 3b,c**).

PBD150 treatment resulted in a significant memory improvement of TASD-41 mice, but not of wild-type littermates, as measured by the freezing time in contextual fear conditioning ($P < 0.05$; **Fig. 3d**). After tone conditioning, the treated mice showed a tendency toward prolonged freezing, which, however, did not reach statistical significance (with tone: wild type untreated, 31.0%; wild type treated, 26.3%; TASD-41 untreated, 22.7%; TASD-41 treated, 47.3%; $F_{3,32} = 1.657$, $P = 0.1959$). In a Morris water maze, PBD150-treated TASD-41 mice showed reduced escape latency as compared with vehicle-treated mice, resulting in a performance that was virtually identical to that of wild-type littermates on the fourth day of training (**Fig. 3e**). Depending on the statistical analysis, the effect of treatment was significant at the fourth day of training (one-way ANOVA, followed by Newman-Keuls multiple comparison test). The effect lacked statistical significance, however, in factorial ANOVA analyzing the entire time of training. In an accompanying probe trial, all groups behaved similarly when the

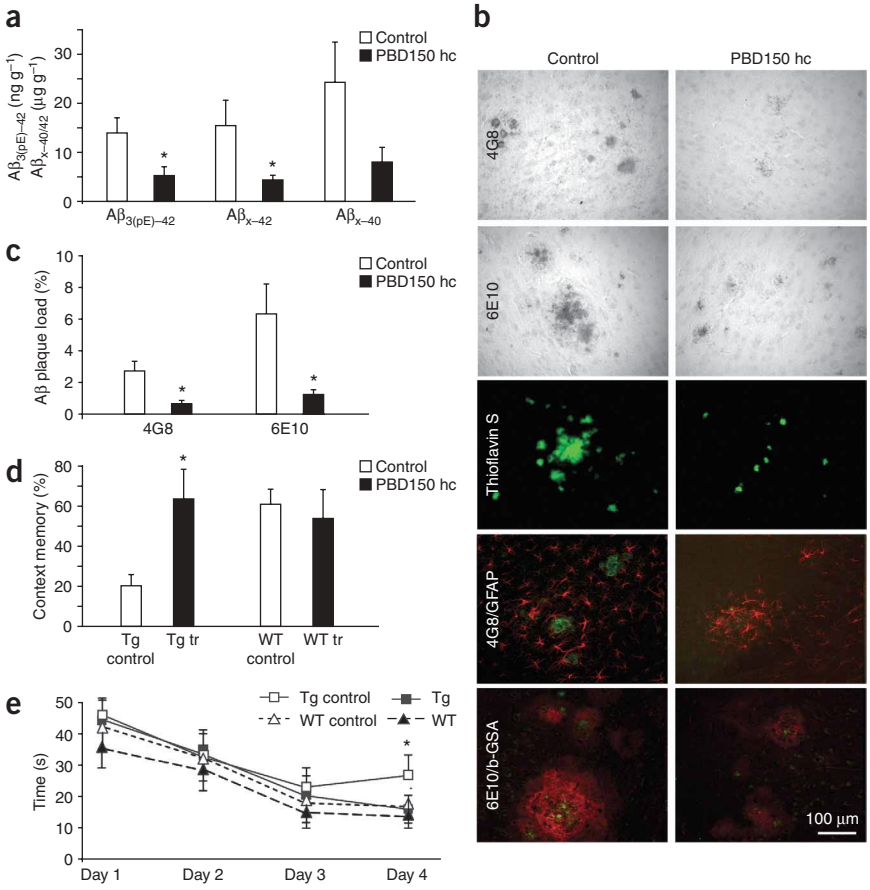

Figure 3 Effects of glutaminyl cyclase inhibition on TASD-41 mice. (**a**) Quantification of Aβ concentrations in the brains of 7-month-old TASD-41 control mice and age-matched littermates treated for 3 months (prophylactic treatment) with PBD150 at a concentration of 7.2 mg (PBD150 hc) per g of food pellets. Groups consisted of male and female mice ($n = 4$–5). (**b**) Immunohistochemical detection of Aβ plaques in 7-month-old control mice and of age-matched littermates treated for 3 months as described in **a**. Top, DAB staining of Aβ plaques with 4G8 and 6E10 antibodies. The reduced Aβ plaque burden was accompanied by diminished gliosis, as shown for astrocytic (GFAP, red fluorescence) and microglial (bio-GSA, red fluorescence) labeling. The scale bar applies to all images. (**c**) The plaque load was significantly reduced, as shown by quantification of histochemical stainings. (**d**) Conditioned fear test performed at the end of the treatment period. There was significantly improved memory (percentage immobile in combined spatial and cued context – percentage in the novel environment) in TASD-41 mice treated with PBD150 as compared with the control group ($n = 7$–8). Treatment of wild-type (WT) mice did not affect memory. Data are expressed as mean ± s.e.m. (*$P < 0.05$ versus control, one-way ANOVA followed by Fisher least-significant difference). Male and female mice were analyzed. (**e**) Morris water maze of PBD150-treated and untreated TASD-41 mice and wild-type littermates. Male and female mice were analyzed ($n = 7$–8). Data are expressed as mean ± s.e.m. (*$P < 0.05$ versus control, one-way ANOVA followed by Newman-Keuls multiple comparison test). A factorial analysis applying two-way ANOVA did not reveal significance for treatment and treatment × time interactions.

platform was removed (**Supplementary Fig. 4** online). PBD150 never affected the performance of wild-type mice or parameters such as the swimming speed, reflecting the specific effect of glutaminyl cyclase inhibition mediated via $A\beta_{3(pE)-42}$ reduction (**Fig. 3e**).

To prove the concept of seeding by pE-Aβ and to further exclude a nonspecific effect of PBD150, we generated transgenic *Drosophila* flies with neuron-specific expression of $A\beta_{1-42}$ or $A\beta_{3(Q)-42}$ (**Fig. 4**). The expression constructs contained the Aβ sequence, which was N-terminally fused to the prepro-sequence of murine thyroliberin (TRH). Liberation of Aβ was accomplished by prohormone convertase processing in the secretory pathway (**Fig. 4a**). The generation of Aβ from these constructs was confirmed by ELISA and urea-PAGE western blotting following expression in S2 *Drosophila* cells (**Fig. 4b**). A 4-week treatment of transgenic flies with PBD150 led to a significant decrease of $A\beta_{3(pE)-42}$ ($P < 0.05$; **Fig. 4c**). On the other hand, total Aβ was not affected in flies expressing $A\beta_{1-42}$, suggesting that PBD150 specifically reduces pE-Aβ (**Fig. 4c**).

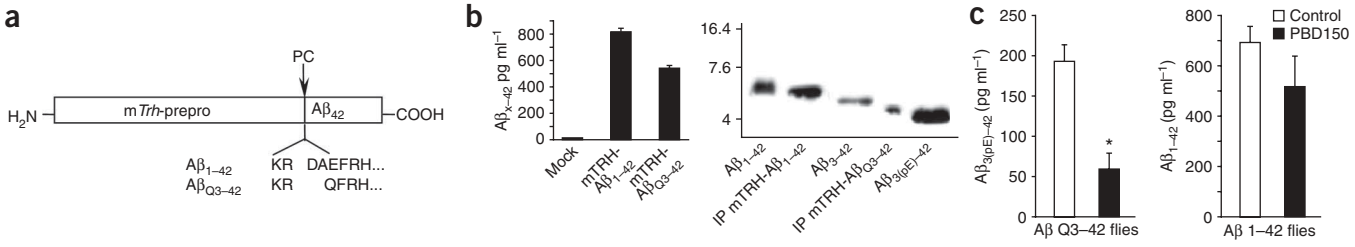

Figure 4 Glutaminyl cyclase inhibition diminishes $A\beta_{3(pE)-42}$ deposition in transgenic *Drosophila* flies. (**a**) Schematic representation of the constructs used for the generation of the N-terminal variants of Aβ in *Drosophila*. The expression constructs consisted of the Aβ sequence, which is fused to the C terminus of the murine TRH prepro-sequence. Processing of the preproprotein in the secretory pathway led to the release of $A\beta_{3(Q)-42}$, the direct precursor of $A\beta_{3(pE)-42}$ or of $A\beta_{1-42}$. (**b**) Expression of the Aβ constructs in S2 *Drosophila* cells. The expression led to significant increases in the Aβ concentrations in the conditioned media, as shown by immunoprecipitation and urea-PAGE followed by immunodetection of $A\beta_{3(pE)-42}$ and $A\beta_{1-42}$. (**c**) Treatment of transgenic *Drosophila* with PBD150. PBD150-supplemented agar (1 mM) was used for application. After 4 weeks of treatment, fly heads were collected and Aβ concentrations were determined by ELISA. A significant effect of treatment was observed with the flies expressing the precursor of $A\beta_{3(pE)-42}$. Data are expressed as mean ± s.e.m. (* $P < 0.05$ versus control).

Previous work[4,6,9,19] has suggested that N-terminally truncated and pE-modified Aβ contributes to the development of Alzheimer's disease, mainly by a boosted aggregation propensity[11,20]. Such N-terminally truncated Aβ peptides are present at very early stages of Alzheimer's disease pathology[4,10] and can be found in the cerebrospinal fluid (CSF) and plasma of individuals suffering from mild cognitive impairment several years before Alzheimer's disease diagnosis[21]. Notably, we found that only $Aβ_{3(pE)–42}$ brain tissue immunoreactivity was associated with Alzheimer's disease pathology, indicating that $Aβ_{3(pE)–42}$ probably contributes to amyloid deposition, thus influencing the progression of the disease (see **Fig. 1**). This has also been observed in early-onset Alzheimer's disease caused by presenilin mutations[5,9].

On the basis of the recently discovered capability of glutaminyl cyclase to catalyze N-terminal pE formation from glutamic acid precursors[13,14], the upregulation of glutaminyl cyclase in brains of individuals with Alzheimer's disease (**Fig. 1**) suggests that glutaminyl cyclase is important for the generation of pE-Aβ peptides. Spontaneous N-terminal pE formation from glutamic acid, as has been recently suggested[22], is very unlikely under physiological conditions, considering that the half life of glutamic acid is years to decades[23].

The coincidence of glutaminyl cyclase overexpression, accumulation of pE-Aβ and progression of neurodegeneration in Alzheimer's disease strongly implies a disease-provoking function of $Aβ_{3(pE)}$. Inhibition of glutaminyl cyclase represents a strategy for reducing $Aβ_{3(pE)–42}$ formation *in vivo*.

In contrast with our recent approach of injecting $Aβ_{3(E)–40}$ into rat brain[24], the Tg2576 and TASD-41 mice showed relatively low levels of $Aβ_{3(pE)–42}$ (see **Fig. 3**), but high levels of $Aβ_{1–40/42}$ (refs. 25,26). In Tg2576 mice, we detected $Aβ_{3(pE)–42}$ by ELISA from 6 months of age onwards, and the first $Aβ_{3(pE)–42}$ immunoreactive plaques appeared at 12 months of age. During aging, $Aβ_{3(pE)–42}$ accumulated, but still represented only 0.1–0.5% of total Aβ. TASD-41 mice developed plaques from 5 months of age onwards and had already revealed behavioral deficits at 6 months of age, which correlates to their relatively high levels of $Aβ_{1–42}$. In preceding experiments, we detected $Aβ_{3(pE)–42}$ at low concentrations, accounting for only 0.5% of the total Aβ. Therefore, these models allowed us to test the seeding hypothesis for $Aβ_{3(pE)–42}$. The reduction of insoluble $Aβ_{3(pE)–42}$ by 50% ($\sim$10 ng per g) resulted in the suppression of the prominent total Aβ by up to 75% ($\sim$30 μg per g; **Figs. 2–4**), whose concentration is more than 1,000-fold higher than pE-Aβ. This finding provides strong evidence for $Aβ_{3(pE)–42}$ as a potential nidus of amyloidogenic aggregation[11,24]. Direct evidence for the high seeding capacity of $Aβ_{3(pE)}$ was also obtained from *in vitro* co-aggregation of $Aβ_{3(pE)–40}$ and $Aβ_{1–40}$ (see also **Supplementary Fig. 5** online). This aggregation process was not affected by the glutaminyl cyclase inhibitor PBD150 used in this study (**Supplementary Fig. 5**). In summary, all experimental data presented here are consistent with the hypothesis of pE-Aβ acting as a seeding peptide species in the amyloid cascade (**Supplementary Fig. 6** online).

In addition, our results have implications for the inherited neurodegenerative amyloidoses familial British dementia and familial Danish dementia, which are caused by stop-codon or frame-shift mutations in the *BRI* gene (also known as *ITM2B*)[27]. The so-called amyloid peptides ADan and ABri account for brain lesions that are similar to those seen in Alzheimer's disease. Virtually all of the deposited BRI peptides in these brains are modified by N-terminal pE. Apparently, these peptides also trigger Aβ deposition, acting as a seeding factor[11,28].

In mouse models with small amounts of $Aβ_{3(pE)–40/42}$ compared with Alzheimer's disease, glutaminyl cyclase inhibition was shown to result in diminished Aβ plaque formation and gliosis, and improved memory. If glutaminyl cyclase inhibition is similarly efficacious in humans, this new approach may prove to be disease-modifying. In conclusion, prevention of pE formation at the N-terminus of peptides by inhibition of glutaminyl cyclase represents a new therapeutic strategy for alleviating amyloidoses caused by the seeding of amyloidogenic peptides.

METHODS

Human brain tissue. The definite diagnosis of Alzheimer's disease for all cases used in this study was based on the presence of neurofibrillary tangles and neuritic plaques in the hippocampal formation and neocortical areas. Case recruitment and autopsy were approved by the Ethical Committee of Leipzig University (License# 063/2000), and informed consent was obtained from all subjects.

mRNA and western blot analysis for glutaminyl cyclase. We carried out quantitative real-time PCR using the QuantiTect Primer Assay for QPCT (QT00013881, Qiagen) as well as the QuantiTect SYBR Green RT-PCR kit (Qiagen). Absolute transcript amounts were determined using external glutaminyl cyclase standard DNA. We normalized against HPRT and GAPDH. For western blot analysis, we homogenized and ultrasonicated the tissue, and detected glutaminyl cyclase using purified rabbit polyclonal antibodies that were raised against human glutaminyl cyclase.

Cell culture. We cultured HEK293 cells in Dulbecco's modified Eagle's medium (10% fetal bovine serum). Cells were co-transfected with the APP695 variant APP-NLE[29] and human glutaminyl cyclase using Lipofectamin2000 (Invitrogen) and were incubated for 24 h in the absence or presence of 0.1 μM and 1.0 μM of PBD150.

Animals. We housed Tg2576 mice (B6/SJL, human APPsw695-transgene) at a 12-h day/12-h night cycle with free access to tap water and food pellets supplemented with either no supplement (control), 2.4 mg PBD150 per g of pellet (low concentration) or 7.2 mg PBD150 per g of pellet (high concentration). Animals were treated for three different periods of time (**Supplementary Fig. 1**). Likewise, TASD-41 mice[26,30] (C57/Bl6 hybrid) were treated via food pellets supplemented with 7.2 mg PBD150 per g of pellet. Animal studies were approved by the local legal authorities 'Regierungspräsidium' of Leipzig (TVV40/04) and the 'Steiermärkische Landesregierung' (Departments 8C and 10A) of Graz (Authorizations 78JO 21_5 – 04 and 78JO 10_6 – 03).

Behavioral testing. For conditioned fear testing, we used two training trials. Mice were placed in an operant chamber, allowed to explore for 2 min and then given an auditory cue for 15 s and a foot shock for 2 s (1.5 mA unpulsed). The mice were returned to the same chamber (context) 24 h after training and freezing behavior (immobility) was recorded for 5 min. We transferred the mice to a novel environment 1 h later and freezing behavior (immobility) was recorded for 3 min. The auditory cue was then presented for 3 min and freezing behavior (immobility) was recorded. Freezing scores are expressed as a percentage for each portion of the test. The Morris water maze task was conducted in three trials on 4 consecutive days. The mouse had to find the hidden, diaphanous target during 1-min trials. After each trial, mice were allowed to rest on the platform for 10–15 s. Escape latency, pathway and presence of the mice in the platform quadrant were quantified. A probe trial, in which the platform was removed, was carried out on the fourth day of training (see **Supplementary Methods** online).

Immunochemical analysis of human and rodent brain samples. We quantified Aβ peptides in 2% SDS and formic acid fractions by sandwich ELISAs (IBL). We carried out immunohistochemical stainings, applying the $Aβ_{3(pE)}$-specific antibody (Clone 6, mouse monoclonal antibody, dilution 1:2,500) and the Aβ-specific antibody (4G8 mouse monoclonal antibody, dilution 1:2,500, Calbiochem) using fixed human tissue (HOPE-fixation, DCS Innovative Diagnostic Systems). For immunodetection, we used a biotinylated mouse-specific IgG (BA 9200, Vector Laboratories), followed by diaminobenzidine staining (Vectastain ABC-Kit, Vector Laboratories). Immunohistochemistry in the mouse brain was performed using the antibodies 6E10 (Chemicon) and

biotinylated antibody 4G8 (Signet), coupled with secondary horseradish peroxidase–conjugated antibodies and the diaminobenzidine reaction. In dual fluorescent immunolabeling procedures, we detected microglial cells with biotinylated lectin *Griffonia simplicifolia* agglutinin isolectin B4 (bio-GSA, Sigma). Depending on the Aβ double-labeling procedure, we visualized astrocytes with mouse GFAP–specific or with rabbit GFAP–specific antibodies (both from Sigma). Brain sections were incubated with cocktails of primary antibodies from different species overnight at 4 °C and then visualized using fluorochromated secondary antibodies.

Generation of transgenic *Drosophila*. We cloned prepro-mTRH-Aβ constructs encoding $A\beta_{1–42}$ and $A\beta_{3(Q)–42}$ into a pUAST expression vector containing P element repeats and *white* as a marker gene. The insertion of the DNA into germ-line chromosomes was mediated by P element transposase. We then selected transgenic lines in the F2 generation. For transgene production, we used a *white*-isogenized *Drosophila* line. Males from five different transgenic lines expressing $A\beta_{1–42}$ or $A\beta_{3(Q)–42}$ were crossed to females of driver line P{GawB}*elav*^{C155} (Bloomington Stock 458). At the age ~50 d, we collected 100 transgenic flies and determined the Aβ content by ELISA.

Statistical analysis. We used one-way ANOVA followed by Tukey's honestly significantly different (HSD) test for analyzing the Aβ ELISAs. We evaluated the conditioned fear data by one-way ANOVA followed by *post hoc* analysis using Fisher protected least-significant difference and Scheffé's tests. For multiple comparisons, $P = 0.5/k$, with k being the number of comparisons that were considered to be significant (Bonferroni-Dunn test). For the Morris water maze data, we applied one- and two-way ANOVA followed by *post hoc* analysis using Newman-Keuls multiple comparison test if significance was obtained in ANOVA.

Note: Supplementary information is available on the Nature Medicine website.

ACKNOWLEDGMENTS

We thank K. Sowa, R. Jendrek, K. Schulz, M. Bornack, E. Scheel and M. Buchholz for technical assistance. The authors would like to express their gratitude to K. Hsiao (University of Minnesota) for kindly providing Tg2576 mice and E. Masliah (University of California, San Diego) for providing the TASD-41 mice. Thanks are due to T.C. Saido (Riken Brain Science Institute) for the gift of the APP-NLE vector. S. Winter maintained and analyzed organotypic brain slice cultures from Tg2576 mice. We are also grateful to J. Heins for statistical analysis and to M.T. Stubbs, K. Glund and M. Hartlage-Rübsamen for helpful discussion. This work was supported by German Federal Department of Education, Science and Technology BMBF grant #3013185 to H.-U.D.

AUTHOR CONTRIBUTIONS

T.H., S.S. and S.R. planned most of the experiments. S.S., H.C., T.H., A.K., D.S. and U.H. conducted most of the biochemical and cell biological investigations. S.S., A.K., W.J., M.F. and M.H. analyzed the human brain tissue. U.Z. and S.R. carried out the Tg2576 mouse experiments. M.P., B.H.-P. and M.W. performed the TASD-41 mouse experiments. D.M. conducted the behavioral analysis of Tg2576. C.L., T.R. and G.R. generated the transgenic *Drosophila* lines. S.R., S.S. and H.-U.D. designed the study and wrote the manuscript. H.-U.D. initiated the research and supervised the program.

COMPETING INTERESTS STATEMENT

The authors declare competing financial interests: details accompany the full-text HTML version of the paper at http://www.nature.com/naturemedicine/.

Published online at http://www.nature.com/naturemedicine/
Reprints and permissions information is available online at http://npg.nature.com/reprintsandpermissions/

1. Hardy, J.A. & Higgins, G.A. Alzheimer's disease: the amyloid cascade hypothesis. *Science* **256**, 184–185 (1992).
2. Iwatsubo, T. *et al.* Visualization of Aβ 42(43) and Aβ 40 in senile plaques with end-specific Aβ monoclonals: evidence that an initially deposited species is Aβ 42(43). *Neuron* **13**, 45–53 (1994).
3. Iwatsubo, T., Mann, D.M., Odaka, A., Suzuki, N. & Ihara, Y. Amyloid beta protein (Aβ) deposition: Aβ 42(43) precedes Aβ 40 in Down syndrome. *Ann. Neurol.* **37**, 294–299 (1995).
4. Saido, T.C. *et al.* Dominant and differential deposition of distinct β-amyloid peptide species, Aβ N3(pE), in senile plaques. *Neuron* **14**, 457–466 (1995).
5. Russo, C. *et al.* Presenilin-1 mutations in Alzheimer's disease. *Nature* **405**, 531–532 (2000).
6. Saido, T.C., Yamao, H., Iwatsubo, T. & Kawashima, S. Amino- and carboxyl-terminal heterogeneity of β-amyloid peptides deposited in human brain. *Neurosci. Lett.* **215**, 173–176 (1996).
7. Naslund, J. *et al.* Relative abundance of Alzheimer Aβ amyloid peptide variants in Alzheimer disease and normal aging. *Proc. Natl. Acad. Sci. USA* **91**, 8378–8382 (1994).
8. Liu, K. *et al.* Characterization of Aβ11–40/42 peptide deposition in Alzheimer's disease and young Down's syndrome brains: implication of N-terminally truncated Aβ species in the pathogenesis of Alzheimer's disease. *Acta Neuropathol.* **112**, 163–174 (2006).
9. Russo, C. *et al.* PE-modified amyloid β-peptides–AβN3(pE)–strongly affect cultured neuron and astrocyte survival. *J. Neurochem.* **82**, 1480–1489 (2002).
10. Saido, T.C. Alzheimer's disease as proteolytic disorders: anabolism and catabolism of β-amyloid. *Neurobiol. Aging* **19**, S69–S75 (1998).
11. Schilling, S. *et al.* On the seeding and oligomerization of pGlu-amyloid peptides (*in vitro*). *Biochemistry* **45**, 12393–12399 (2006).
12. Miravalle, L. *et al.* Amino-terminally truncated Aβ peptide species are the main component of cotton wool plaques. *Biochemistry* **44**, 10810–10821 (2005).
13. Schilling, S., Hoffmann, T., Manhart, S., Hoffmann, M. & Demuth, H.-U. Glutaminyl cyclases unfold glutamyl cyclase activity under mild acid conditions. *FEBS Lett.* **563**, 191–196 (2004).
14. Cynis, H. *et al.* Inhibition of glutaminyl cyclase alters pE formation in mammalian cells. *Biochim. Biophys. Acta* **1764**, 1618–1625 (2006).
15. Pohl, T., Zimmer, M., Mugele, K. & Spiess, J. Primary structure and functional expression of a glutaminyl cyclase. *Proc. Natl. Acad. Sci. USA* **88**, 10059–10063 (1991).
16. Sykes, P.A., Watson, S.J., Temple, J.S. & Bateman, R.C.J. Evidence for tissue-specific forms of glutaminyl cyclase. *FEBS Lett.* **455**, 159–161 (1999).
17. Buchholz, M. *et al.* The first potent inhibitors for human glutaminyl cyclase: synthesis and structure-activity relationship. *J. Med. Chem.* **49**, 664–677 (2006).
18. Jacobsen, J.S. *et al.* Early-onset behavioral and synaptic deficits in a mouse model of Alzheimer's disease. *Proc. Natl. Acad. Sci. USA* **103**, 5161–5166 (2006).
19. Piccini, A. *et al.* β-amyloid is different in normal aging and in Alzheimer disease. *J. Biol. Chem.* **280**, 34186–34192 (2005).
20. Pike, C.J., Overman, M.J. & Cotman, C.W. Amino-terminal deletions enhance aggregation of β-amyloid peptides *in vitro*. *J. Biol. Chem.* **270**, 23895–23898 (1995).
21. Vanderstichele, H. *et al.* Amino-truncated β-amyloid42 peptides in cerebrospinal fluid and prediction of progression of mild cognitive impairment. *Clin. Chem.* **51**, 1650–1660 (2005).
22. Hashimoto, T. *et al.* CLAC: a novel Alzheimer amyloid plaque component derived from a transmembrane precursor, CLAC-P/collagen type XXV. *EMBO J.* **21**, 1524–1534 (2002).
23. Yu, L. *et al.* Investigation of N-terminal glutamate cyclization of recombinant monoclonal antibody in formulation development. *J. Pharm. Biomed. Anal.* **42**, 455–463 (2006).
24. Schilling, S. *et al.* Inhibition of glutaminyl cyclase prevents pGlu-Aβ formation after intracortical/hippocampal microinjection *in vivo*/*in situ*. *J. Neurochem.* **106**, 1225–1236 (2008).
25. Kawarabayashi, T. *et al.* Age-dependent changes in brain, CSF, and plasma amyloid (β) protein in the Tg2576 transgenic mouse model of Alzheimer's disease. *J. Neurosci.* **21**, 372–381 (2001).
26. Rockenstein, E., Mallory, M., Mante, M., Sisk, A. & Masliah, E. Early formation of mature amyloid-β protein deposits in a mutant APP transgenic model depends on levels of Aβ (1–42). *J. Neurosci. Res.* **66**, 573–582 (2001).
27. Ghiso, J. *et al.* Chromosome 13 dementia syndromes as models of neurodegeneration. *Amyloid* **8**, 277–284 (2001).
28. Tomidokoro, Y. *et al.* Familial Danish dementia: co-existence of Danish and Alzheimer amyloid subunits (ADan AND Aβ) in the absence of compact plaques. *J. Biol. Chem.* **280**, 36883–36894 (2005).
29. Shirotani, K., Tsubuki, S., Lee, H.J., Maruyama, K. & Saido, T.C. Generation of amyloid beta peptide with pE at position 3 in primary cortical neurons. *Neurosci. Lett.* **327**, 25–28 (2002).
30. Hutter-Paier, B. *et al.* The ACAT inhibitor CP-113,818 markedly reduces amyloid pathology in a mouse model of Alzheimer's disease. *Neuron* **44**, 227–238 (2004).